

Numerical Tissue Characterization in MS via Standardization of the MR Image Intensity Scale

Yulin Ge, MD, Jayaram K. Udupa, PhD,* Lázló G. Nyúl, MSc, Luogang Wei, MSc, and Robert I. Grossman, MD

Image intensity standardization is a recently developed postprocessing method that is capable of correcting the signal intensity variations in MR images. We evaluated signal intensity of healthy and diseased tissues in 10 multiple sclerosis (MS) patients based on standardized dual fast spin-echo MR images using a numerical postprocessing technique. The main idea of this technique is to deform the volume image histogram of each study to match a standard histogram and to utilize the resulting transformation to map the image intensities into standard scale. Upon standardization, the coefficients of variation of signal intensities for each segmented tissue (gray matter, white matter, lesion plaques, and diffuse abnormal white matter) in all patients were significantly smaller (2.3–9.2 times) than in the original images, and the same tissues from different patients looked alike, with similar intensity characteristics. Numerical tissue characterizability of different tissues in MS achieved by standardization offers a fixed tissue-specific meaning for the numerical values and can significantly facilitate image segmentation and analysis. J. Magn. Reson. Imaging 2000; 12:715–721. © 2000 Wiley-Liss, Inc.

Index terms: image standardization; magnetic resonance imaging; multiple sclerosis

QUANTITATIVE ASSESSMENT of multiple sclerosis (MS) via MRI has been widely employed in assessing the disease process and activity (1). A variety of computer algorithms have been developed for this quantitative analysis (2–5), all of which, at present, utilize signal intensity (SI) for delineating lesions via T1- and dual spin-echo or dual fast spin-echo (FSE) T2-weighted protocols. Unfortunately, there is considerable variation in the actual SI range for tissues observed in MS patients, depending on several factors including the magnetic field strength and homogeneity, the T1 to T2 weighting, data acquisition method, and slice thickness (6–9). The SI values may vary even for the same patient, in the same body region, in the same protocol, and on the same scanner.

It has also been observed that this variation of SI increases in FSE images compared with conventional

spin-echo images, although FSE has clear advantages in monitoring MS due to its reduced acquisition time (10–13). The SI variations pose considerable challenges to any lesion segmentation method (4). They also cause difficulties in setting window level and width for displaying and viewing the images on computer monitors and for filming the images with proper exposure.

A postacquisition image processing method (14) has recently been developed in order to achieve standardization of intensity values, independent of the patient, the scanner, and the time of scanning. The main motivation for this method comes not particularly from MS image analysis but from the need to make MR image segmentation methods in different applications more robust to SI variations. This method (14) is based on transforming the intensity histogram of each given volume image into a “standard” histogram. The “standard” histogram parameters required for the deformation are determined in a training phase. There is a significant gain in the similarity of the resulting images by this method of transforming the individual intensity scale to the standard scale (14). There have been other attempts at standardization using phantoms (15,16). Since there are no special acquisition requirements for our method, it is applicable to all acquired images.

The brain has a graded SI composition in MS patients within each tissue region including white matter (WM), gray matter (GM), and lesion plaques. Not all abnormalities in MS will result in MS-like demyelinated macroscopic plaques on proton density (PD)- and T2-weighted images (17,18) because of various stages of lesion development and tissue damage. In contrast to normal appearing WM (19), there are also the nonplaque (microscopic) lesions, which manifest with subtle signal intensity changes in WM; they can be seen on high-resolution PD- and T2-weighted images only by close scrutiny. We call these tissues diffuse abnormal white matter (DAWM).

Lesion quantification in the past has been limited to the macroscopic MS plaques in published methods (20). This is because of the poor contrast between nonplaque microscopic lesions and the brain, particularly in the subcortical regions, and more importantly, because of the considerable SI variations in these regions from study-to-study. In this paper, we examine the possibility of utilizing the standardization method in conventional T2 and PD images to examine healthy as well

Department of Radiology, Hospital of the University of Pennsylvania, Philadelphia, Pennsylvania 19104-6021.

*Address reprint requests to: J.K.U., MIPG, 4th Floor Blockley Hall, 423 Guardian Drive, Philadelphia, PA 19104-6021.

E-mail: jay@mipg.upenn.edu

Received February 1, 2000; Accepted June 8, 2000.

as diseased tissues in MS patients. If this effort is successful, it will also free us from the special acquisition efforts aimed at measuring the T2 relaxation time (21–24). We demonstrate that the standardized images resulting from our methods will exhibit uniformity of intensity values and therefore will enable us to characterize numerically different tissue regions: GM, WM, macroscopic plaques, and DAWM in MS patients. We also show that this tissue-specific characterization is not possible in the original (nonstandardized) images. This is one of the reasons why segmentation methods for detecting lesions require considerable per-study user input.

MATERIALS AND METHODS

Ten patients, nine women and one man, aged from 26 to 37 (mean, 32.6) years, with clinically definite relapsing-remitting MS as defined by Poser criteria (25) were evaluated. The studies for these patients were selected randomly from our image database. All MR images were acquired with a 1.5-T Scanner (Signa, GE Medical Systems, Milwaukee, WI) and with a quadrature transmitter/receiver head coil. The protocol consisted of axial PD- and T2-weighted dual FSE imaging with interleaved contiguous 3-mm-thick slices. The parameters were as follows: TR/TE_{eff} 2500/18 and 90 msec, echo train length 8, number of excitations (NEX) 1, matrix size 192 × 256, and field of view (FOV) 22 cm².

All acquired MR image data were transferred directly to the computer systems of the Medical Image Processing Group. We used the 3DVIEWS software system (26) for image processing. All processing operations were carried out on a SunSparc 20 workstation (Sun Microsystems, Mountain View, CA). For the numerical characterization of GM, WM, plaques, and DAWM tissue regions in MS patients, and to demonstrate the effectiveness of this characterization, the following steps were executed for each patient study.

Step 1. Standardization of the MR Images

Each given volume image V_{PDi} and V_{T2i} , $1 \leq i \leq 10$, was subjected to an intensity scale standardization transformation (14). The aim of this transformation was to make the voxels containing the same tissue have as similar intensities as possible in all transformed images. It is based on deforming the intensity histogram of each given whole-volume image into a “standard” histogram. This was achieved in two steps, a training step executed only once for each given protocol (eg, FSE PD, T2) and body region (eg, head), and a transformation step executed for each volume image.

In the training step, which was performed in the previous study (14) based on 10 separate MS data sets, certain landmarks of a standard histogram (for the body region and protocol under consideration) were estimated from a given set of volume images. The landmarks used in this application were a low and a high percentile and the median of the hump corresponding to the foreground (the head). We utilized the parameters that were already determined by training for this FSE T2 and PD protocol previously for other projects based on other data sets in our database. The data from dif-

ferent patients, different scanners, and different hospitals (MR scanners) were utilized for validating this method (14) by qualitative and quantitative analysis.

In the transformation step, the actual intensity transformation from the intensity scale of the input volume image to the standard scale was computed by mapping the landmarks determined from the histograms. This step usually results in a deformation of the histogram of the input volume image and a concomitant nonlinear intensity transformation. No two intensities in the input image are merged, and the relationship among intensities in the different tissue regions in the input images is maintained in the output image (14). Both training and transformation are completely automatic. The algorithms and the theory associated with this method are described in detail in ref. 14 with illustrations considering many MRI protocols for many body regions and data from different hospitals. This step outputs two new standardized volume images denoted V_{PDi}^s and V_{T2i}^s , $1 \leq i \leq 10$.

Step 2. Segmentation of Normal and Abnormal Tissues (GM, WM, Lesion Plaques, and DAWM)

First, the MS lesion plaques were segmented each as a three-dimensional (3D) fuzzy object by an algorithm using fuzzy connectedness (4) utilizing V_{PDi}^s and V_{T2i}^s . As a byproduct of this method, the brain parenchyma, cerebrospinal fluid (CSF), WM, and GM were also segmented. The voxels belonging to MS lesion plaques were removed from the WM and GM masks, resulting in “pure” 3D tissue masks for these regions.

DAWM usually appears with a slightly higher SI than normal WM on both PD and T2 images in the subcortical area. Our effort in this work is to try to understand the SI characteristics of DAWM in a standard manner so that more automated methods to segment these tissue regions based on these SI characteristics can be devised in the future. Therefore, a trained neuroradiologist (Y.G.) carefully painted the abnormal tissue regions on slice image displays to get a DAWM mask using the manual painting functions of 3DVIEWS (26). The segmented normal WM and MS plaques were then subtracted from the painted masks to make sure that only DAWM is utilized in the evaluation. At the end of this step 2, thus, we had a 3D mask for each of WM, GM, plaques, and DAWM for each pair of volume images (V_{PDi}^s , V_{T2i}^s). The exact same masks are also utilized on the corresponding pair of original images (V_{PDi} , V_{T2i}) for evaluating SI distributions. In this fashion, all tissue regions identified in the standardized images are also considered in exactly the same manner voxel-per-voxel in the original images.

Step 3: Measurement of the SI

For each of the volume images V_{PDi} , V_{T2i} , V_{PDi}^s and V_{T2i}^s , for $1 \leq i \leq 10$, and within each of the segmented tissue regions GM, WM, plaques, and DAWM, the signal intensities were determined. Their statistics over 10 data sets including mean, standard deviation (SD), percent coefficient of variation (%CV), and the 95% confidence interval (CI) before and after standardization were computed. The SI distributions (histograms) for the differ-

Table 1
Signal Intensity Measurements of Four Tissues on PD Images in Ten Patients*

	Standardized PD				Original PD			
	GM	WM	LP	DAWM	GM	WM	LP	DAWM
Mean	2496.0	2200.5	2871.3	2397.6	735.8	655.6	832.0	709.8
SD	43.4	25.1	119.5	51.4	75.0	66.4	85.4	73.0
Median	2501.5	2206.5	2865.0	2395.0	728.0	653.0	842.0	703.5
% CV	1.7	1.1	4.2	2.1	10.2	10.1	10.3	10.3
CI lower	2469.1	2184.9	2797.2	2365.7	689.3	614.4	779.1	664.6
CI higher	2522.9	2216.1	2945.4	2429.5	782.3	696.8	884.9	755.0

*SD = standard deviation, CI = 95% confidence interval, % CV = percent coefficient of variation, GM = gray matter, WM = white matter, LP = lesion plaques, DAWM = diffuse abnormal white matter.

ent tissue regions before and after standardization were computed and plotted to give a visual presentation of the inter- and inpatient SI variations within each tissue region.

RESULTS

Tables 1 and 2 display the mean, median, SD, %CV, and CI values for each tissue region for both PD and T2 images over the 10 data sets. The %CV of SI was reduced by a factor of 2.3–9.2 after standardization compared with the original images. This reduction is the greatest for WM and GM and not as large for the more diffuse and fuzzily defined DAWM and plaques. The 95% CIs indicate that there is very little overlap in the SI ranges for various tissues among patients after standardization, while the overlap before standardization is substantial. The distributions of SI for the different tissues are displayed in Figs. 1–4. Figures 1 and 2 show SI distributions for WM in each of the 10 studies in the PD images before and after standardization, respectively. The SI distributions for each tissue in the different patients are haphazard and chaotic before standardization (Fig. 1), whereas they concur after standardization (Fig. 2). Figures 3 and 4 show SI distributions for each of GM, WM, DAWM, and plaques pooling all 10 PD studies together, before, and after standardization. That is, each distribution represents the histogram of SIs for one tissue in all 10 studies. The SI distribution for each tissue appears quite chaotic before standardization (Fig. 3) but demonstrates a typical Gaussian-like form after standardization (Fig. 4). Other individual tissue SI distributions in PD and T2 images not displayed here exhibited patterns analogous to those in Figs. 1 and 2.

The mean SIs were significantly higher in plaques with a relatively larger %CV than in all other tissues after standardization. The mean SI of plaques was raised by 30.5% in standardized PD images and by 66.5% in standardized T2 images compared with WM, by 19.8% in standardized PD images, by 45.7% in standardized T2 images compared with DAWM, and by 15% in standardized PD images and by 36.8% in standardized T2 images compared with GM. However, the difference was greater in T2 images than in PD images. In contrast, the difference between DAWM and GM after standardization was the smallest, and there was some overlap of the SI range, as can be seen in Fig. 4. Note that such an assessment of SI differences for the different tissues before standardization is completely meaningless, as clearly demonstrated by Fig. 3.

To illustrate further the numerical characterizability achieved by standardization, we display in Fig. 5 a slice from each of three PD studies in three patients and the corresponding thresholded binary images before and after standardization for selecting the WM region. The threshold intervals were defined to be [CI lower, CI higher] where CI was the 95% confidence interval of SI for WM over all 10 studies. Clearly, the same tissue region is selected by the fixed threshold interval after standardization in all three studies (Fig. 5b), whereas different tissues are highlighted in the different studies by the fixed threshold interval determined from the SI distribution before standardization (Fig. 5c).

DISCUSSION

This study demonstrates the usefulness of the standardization of MR image intensity of specific tissues in a numerical way in MS patients. From Tables 1 and 2,

Table 2
Signal Intensity Measurements of Four Tissues on T2 Images in Ten Patients*

	Standardized T2				Original T2			
	GM	WM	LP	DAWM	GM	WM	LP	DAWM
Mean	2004.2	1646.8	2742.6	1882.2	355.6	289.0	496.1	331.1
SD	53.2	47.4	176.7	73.6	53.2	47.2	80.9	57.5
Median	2004.5	1648.5	2696.5	1891.5	370.0	305.5	520.0	350.5
% CV	2.7	2.9	6.4	3.9	15.0	16.3	16.3	17.4
CI lower	1971.2	1617.4	2633.1	1836.6	322.6	259.7	446.0	295.5
CI higher	2037.2	1676.2	2852.1	1927.8	388.6	318.3	546.2	366.7

*SD = standard deviation, CI = 95% confidence interval, % CV = percent coefficient of variation, GM = gray matter, WM = white matter, LP = lesion plaques, DAWM = diffuse abnormal white matter.

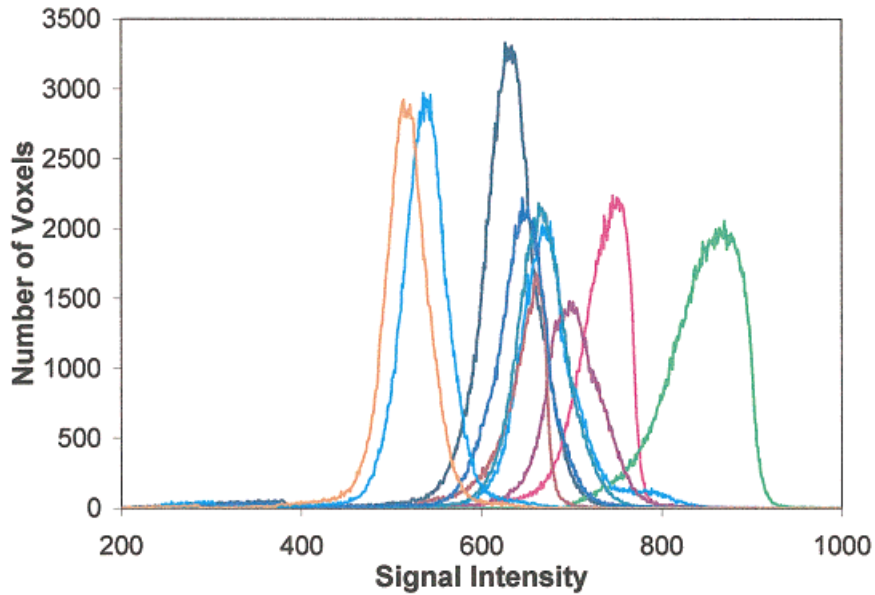


Figure 1. Signal intensity distributions of one tissue (white matter) in the original PD images in 10 patients.

it is clear that the %CV of SI was significantly reduced (2.3–9.2 times) in all standardized PD/T2 images compared with original images. There is very little overlap in the SI ranges (95%CI) after standardization for various tissues among patients compared with that before standardization. This preliminary study shows that the image intensity range for each MS brain tissue from different patients looks alike, with similar intensity characteristics after standardization. This is further illustrated in Figs. 1–5. Image standardization will not only improve the degree of automation and reliability of segmentation of these tissues in the future but also enhance our understanding of the intensity characteristics of given tissues in the MS brain.

MR imaging is an important diagnostic test for evaluating disease evolution and drug efficacy in MS patients. PD and T2-weighted MR images remain the most sensitive protocols for lesion detection (27) in routine MRI. However, FSE T2-weighted image intensities are quite a complex function of the interindividual and interequipment variations. This is due to the dependence of the induced currents and the spatial inhomogeneity of the excitation field on the geometry and electrical properties of the subject as well as on the pulse sequence and coil polarization (28,29). The standardization method (14) is applicable to any images independent of patients, equipment, and protocol to achieve the same consistent meaning for the image intensities.

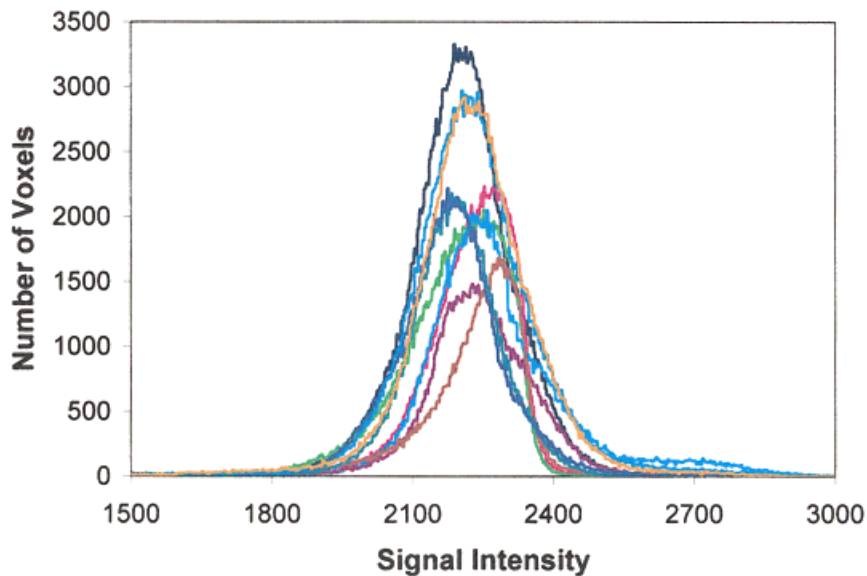


Figure 2. Signal intensity distributions of one tissue (white matter) in the standardized PD images in 10 patients.

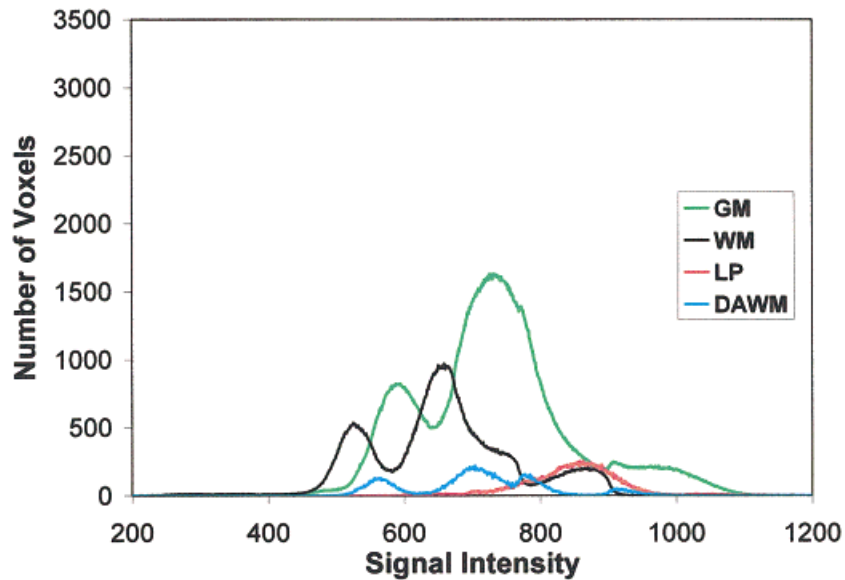


Figure 3. Combined signal intensity distribution in 10 patients for each of four tissues on original PD images. Note that there are several peaks for each tissue and a considerable overlap among tissues. The distributions for lesion plaques (LP) and DAWM have been magnified 5 times for a better display because of the small number of voxels in these regions.

This post hoc method does not require specialized acquisition protocols or calibration phantoms and is therefore applicable to images already acquired without any calibration technique in mind. The consistency of the brightness level and contrast of images is also considerably improved after standardization (14). This permits standardizing and fixing “windows” by protocol, body region, and tissue regions. This will minimize or eliminate the human interaction required in the per-case manual window adjustments that are currently required in visualizing MR images on physician viewing

stations. The scanner-dependent intra- and interpatient intensity variations are substantially reduced after standardization.

This image standardization method is simple, fast, easy to implement, and completely automatic. The standardization step takes only a few seconds per study on a SunSparc 20 workstation. Upon standardization in our study, tissues on both PD and T2 images in different patients had a significantly reduced %CV and overlap (Tables 1, 2). This is why the SI distribution over all 10 patients for each tissue appears quite chaotic

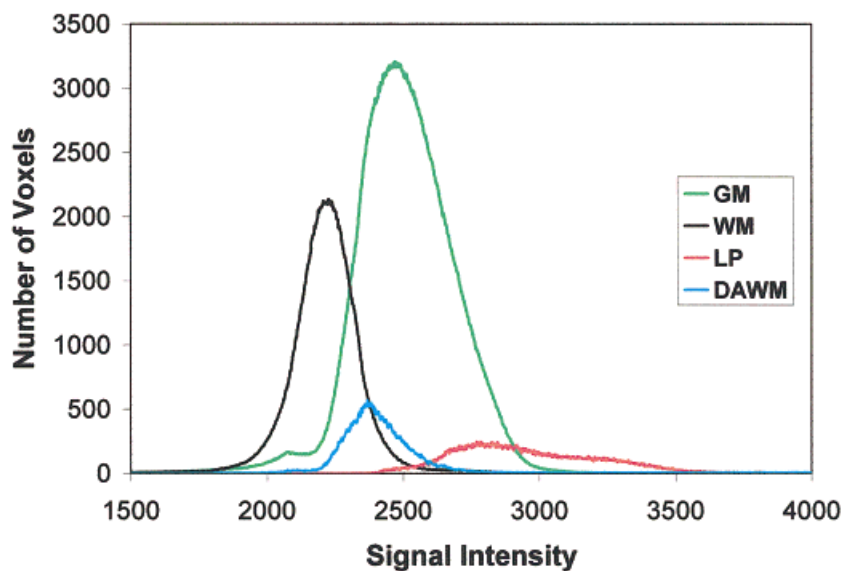


Figure 4. Combined signal intensity distribution in 10 patients for each of four tissues on standardized PD images. Note that there is only one peak for each tissue and less overlap among tissues compared with the distributions for the original images. The distributions for lesion plaques (LP) and DAWM have been magnified 5 times for a better display because of the small number of voxels in these regions.

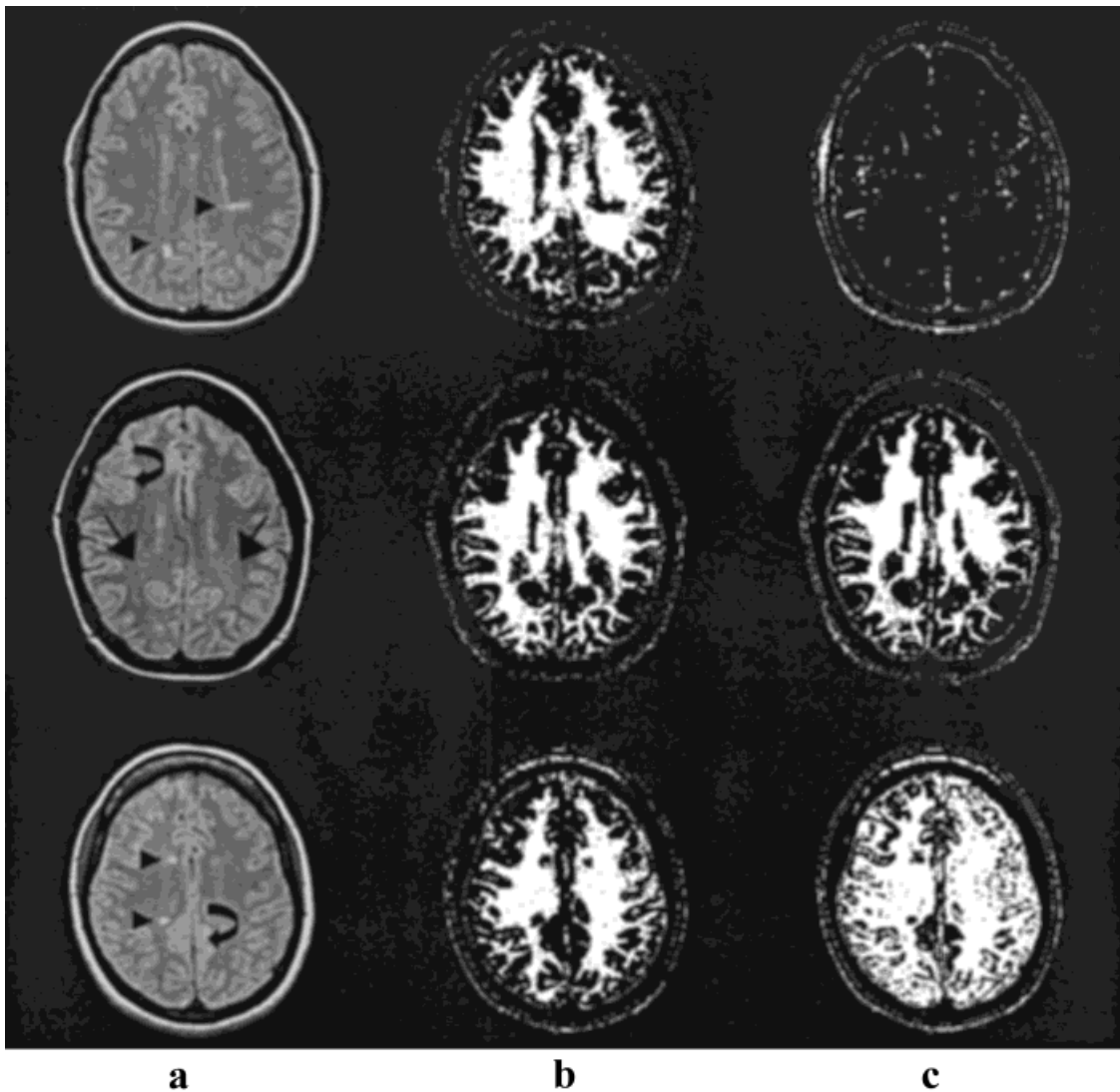


Figure 5. A visual illustration of numerical tissue characterizability. The region corresponding to the threshold interval [CI lower, CI higher] in three MS patients is highlighted, where CI is 95% confidence interval of SI of white matter over all 10 studies. **a:** Original PD images from three different studies. **b:** The WM tissue region is correctly highlighted in all three patients after standardization. Note that plaques (arrowheads), DAWM (arrows), and GM (curved arrows) were not highlighted in the segmented images. **c:** The highlighted tissue region does not represent WM in the first and third study.

before standardization (Fig. 3) but demonstrates a typical Gaussian-like form after standardization (Fig. 4). Figure 5 further illustrates visually the numerical tissue characterizability achieved that is demonstrated in Tables 1 and 2 and Figs. 1–4. The same type of tissue is highlighted by a fixed threshold interval after standardization (Fig. 5b), whereas, before standardization, such fixed numerical tissue meaning does not exist (Fig. 5c).

We are not suggesting that after standardization tissue regions can be segmented by thresholding. Our only aim behind Fig. 5 is to demonstrate the numerical tissue characterizability of tissue regions independent of patients/studies. Because of the ubiquitous noise, blurring, and graded composition of tissues, segmentation by fixed thresholding is rarely meaningful in medical imaging. Our point is that the SI characteristics have significantly improved from Figs. 1 and 3 to 2 and 4. Although there is an overlap in the SI distributions

for the different tissues (for example, between WM and DAWM, and between GM and DAWM), the spatial contiguity and arrangement of voxels in each of these regions can be exploited by techniques such as fuzzy connectedness (4) to develop effective segmentation strategies. We are pursuing these directions at present.

The graded intensity of different tissues in an MS brain on dual-echo FSE T2-weighted images comes from, in addition to noise and blurring, the complicated demyelinating process that is based largely on the extent of scarring and inflammatory activity (30). Since the standardized scale was based on a smooth deformation of the histogram, this graded intensity of various tissues is not changed after standardization. In some cases, MS microscopic lesions appear slightly hyperintense on PD- and T2-weighted images in the sub-cortical area. Although the neuropathological understanding of DAWM is still poor, the presence of

abnormal SI on PD- and T2-weighted images is a frequent finding.

Our intention behind this study was to compare the different ranges of SI from MS brains after image standardization. Among the four tissues, the mean SI of plaques was the highest and that of WM the lowest. We are not surprised that the mean SI of DAWM is between that of WM and GM on both PD- and T2-weighted images after standardization. The bigger %CV in plaques and DAWM than in GM and WM also indicates the complicated pathological conditions in diseased MS tissues. However, we found that the SIs of DAWM and GM are the closest. That is why segmentation of these tissues using these values as thresholds will always show some overlaps between GM and DAWM. Since the mean SI of DAWM is much lower than that of plaques (19.8% on PD, and 45.7% on T2 standardized images), DAWM has not usually been accounted for in past lesion load measurements based on T2 images. This may explain the poor correlation repeatedly observed in most reported studies between T2 lesion load and clinical parameters.

In conclusion, the MR image standardization method of (14) is a promising technique that may permit direct and accurate characterization of healthy and diseased tissues in MS patients as shown in this paper. The different intensity ranges after standardization for DAWM and WM, as well as for plaques, support the notion that the WM abnormality in MS is a diffuse and fuzzy phenomenon ("fuzzy" here refers to the graded intensity that exists in each tissue region rather than one fixed intensity). Finally, the method of characterization presented here is also applicable to the study of other neurological diseases via MRI. The standardized intensities may play a role similar to that of magnetization transfer ratio (31), which has been shown to provide a numerical characterization of macroscopic as well as microscopic MS disease.

REFERENCES

- Grossman RI, McGowan JC. Perspective of multiple sclerosis. *AJNR* 1998;19:1251-1265.
- Wells III WM, Grimson WEL, Kikinis R, Jolesz FA. Adaptive segmentation of MRI data. *IEEE Trans Med Imaging* 1996;15:429-442.
- Wicks DA, Tofts PS, Miller DH, et al. Volume measurement of multiple sclerosis lesions with magnetic resonance images. *Neuroradiology* 1992;34:475-479.
- Udupa JK, Wei L, Samarasekera S, et al. Multiple sclerosis lesion quantification using fuzzy-connectedness principles. *IEEE Trans Med Imaging* 1997;16:598-609.
- Kamber M, Shingal R, Collins DL, Francis GS, Evans AC. Model-based 3-D segmentation of multiple sclerosis lesions in magnetic resonance brain images. *IEEE Trans Med Imaging* 1995;14:442-453.
- Keiper MD, Grossman RI, Hirsch JA, et al. MR identification of white matter abnormalities in multiple sclerosis: a comparison between 1.5T and 4T. *AJNR* 1998;19:1489-1493.
- Filippi M, Rocca MA, Gasperini C, et al. Interscanner variation in brain MR lesion load measurements in multiple sclerosis using conventional spin-echo, rapid relaxation-enhanced, and fast-FLAIR sequences. *AJNR* 1999;20:133-137.
- Simon JH, Scherzinger A, Raff U, Li X, et al. Computerized method of lesion volume quantitation in multiple sclerosis: error of serial studies. *AJNR* 1997;18:580-582.
- Molyneux PD, Tubridy N, Parker GJM, et al. The effect of section thickness on MR lesion detection and quantification in multiple sclerosis. *AJNR* 1998;19:1715-1720.
- Thorpe JW, Halpin SF, MacManus DG, et al. A comparison between fast and conventional spin-echo in the detection of multiple sclerosis lesions. *Neuroradiology* 1994;36:388-392.
- Yousry TA, Filippi M, Becker C, et al. Comparison of SE, FSE, fast-FLAIR and TGSE sequences in detecting multiple sclerosis lesions. *AJNR* 1997;18:959-963.
- Bastinaello S, Bozzao A, Paolillo A, et al. Fast spin-echo and fast fluid-attenuated inversion-recovery versus conventional spin-echo sequences for MR quantification of multiple sclerosis. *AJNR* 1997;18:699-704.
- Rovaris M, Gawne-Cain ML, Wang L, Miller DH. A comparison of conventional and fast spin-echo sequences for the measurement of lesion load multiple sclerosis using a semiautomated contouring technique. *Neuroradiology* 1997;39:161-165.
- Nyul LG, Udupa, JK. On standardizing the MR image intensity scale. *Magn Reson Med* 1999;42:1072-1081.
- Edelstien WA, Bottomley PA, Pfeifer LM. A signal-to-noise calibration procedure for NMR imaging systems. *Med Phys* 1984;11:180-185.
- Yamamoto T, Nambu T, Miyasaka K, Morita Y. Accurate and practical calibration of MR signal intensities by the new transmission amplitude method: application of the numerical diagnosis to MRI. *Radiology* 1998;209P:582.
- Dousset V, Grossman RI, Ramer KN, et al. Experimental allergic encephalomyelitis and multiple sclerosis: lesion characterization with magnetization transfer imaging [published erratum appears in *Radiology* 1992;183:878]. *Radiology* 1992;182:483-191.
- Rooney WD, Goodkin DE, Schuff N, et al. ¹HMRI of normal appearing white matter in multiple sclerosis. *Multiple Sclerosis* 1997;3:231-237.
- Miller DH, Johnson G, Tofts PS, MacManus D, McDonald WI. Precise relaxation time measurements of normal-appearing white matter in inflammatory central nervous system disease. *Magn Reson Med* 1989;11:331-336.
- Phillips MD, Grossman RI, Miki Y, et al. Comparison of T2 lesion volume and magnetization transfer ratio histogram analysis of atrophy and measures of lesion burden in patients with multiple sclerosis. *AJNR* 1998;19:1055-1060.
- Larsson HBW, Fredericksen J, Kjør L, Henriksen O, Olesen J. In vivo determination of T1 and T2 in the brain of patients with severe but stable multiple sclerosis. *Magn Reson Med* 1988;7:44-55.
- Armpach JP, Gounot D, Rumbach L, et al. In vivo determination of multi-exponential T2 relaxation in the brain of patients with multiple sclerosis. *Magn Reson Imaging* 1991;9:107-113
- Larsson HBW, Barker GJ, MacKay A. Nuclear magnetic resonance relaxation in multiple sclerosis. *J Neurol Neurosurg Psychiatry* 1998;64:S70-S76.
- Paty DW, McFarland H. Magnetic resonance techniques to monitor the long term evolution of multiple sclerosis pathology and to monitor definitive clinical trials. *J Neurol Neurosurg Psychiatry* 1998;64:S47-S51.
- Poser CM, Paty DW, Scheinberg L, et al. New diagnostic criteria for multiple sclerosis: guidelines for research protocols. *Ann Neurol* 1983;13:227-231.
- Udupa JK, Odhner D, Samarasekera S, et al. 3DVIWENIX: an open, transportable, multidimensional, multimodality, multiparametric imaging software system. *SPIE Proc* 1994;2164:58-73.
- Siewert B, Patel MR, Mueller MF, et al. Brain lesions in patients with multiple sclerosis: detection with echo-planar imaging. *Radiology* 1995;196:765-771.
- Whittal KP, Mackay AL, Craeb DA, et al. In vivo measurement of T2 distributions and water contents in normal human brain. *Magn Reson Med* 1997;37:34-43.
- Sled JG, Pike GB. Standing-wave and RF penetration artifacts caused by elliptic geometry: an electrodynamic analysis of MRI. *IEEE Trans Med Imaging* 1998;17:653-662.
- Lassmann H. Neuropathology in multiple sclerosis: new concepts. *Multiple Sclerosis* 1998;4:93-98.
- van Buchem MA, McGowan JC, Kolson DL, Polansky M, Grossman RI. Quantitative volumetric magnetization transfer analysis in multiple sclerosis: estimation of macroscopic and microscopic disease burden. *Magn Reson Med* 1996;36:632-636.